



Type-III see-saw: Search for triplet fermions in final states with multiple leptons and fat-jets at 13 TeV LHC



Saiyad Ashanujjaman ^{a,b,*}, Kirtiman Ghosh ^{a,b}

^a Institute of Physics, Bhubaneswar, Sachivalaya Marg, Sainik School, Bhubaneswar 751005, India

^b Homi Bhabha National Institute, Training School Complex, Anushakti Nagar, Mumbai 400094, India

ARTICLE INFO

Article history:

Received 16 November 2021

Received in revised form 4 January 2022

Accepted 6 January 2022

Available online 10 January 2022

Editor: A. Ringwald

Keywords:

Type-III see-saw

Triplet fermions

Multi-lepton final states

Fat-jet signatures

ABSTRACT

The type-III see-saw model holding out a riveting rationale for the minuscule neutrino masses caters for a well-to-do phenomenology at the Large Hadron Collider (LHC). Several searches targetting the triplet fermions have been performed at the LHC. Not only are the signals for the leptonic final states considered in these searches suppressed by the branching fractions of the Standard Model (SM) bosons, but they are also beset with considerably large SM backgrounds. Thus, these searches are deemed not to be sensitive enough in probing the triplet fermions much heavier than 1 TeV. To this end, we perform a search for the triplet fermions in final states with multiple leptons and fat-jets that are cleaner than the usual LHC searches and allow kinematic reconstruction of the triplets. After performing a systematic and comprehensive analysis with seven distinct final states, we project the required luminosities for both 3σ and 5σ discoveries of the triplet fermions as a function of their mass. The triplet fermions with mass as large as 1265 (1380) and 1480 (1600) GeV could be discovered with 5σ (3σ) significance at 500 and 3000 fb^{-1} luminosities, respectively.

© 2022 The Author(s). Published by Elsevier B.V. This is an open access article under the CC BY license (<http://creativecommons.org/licenses/by/4.0/>). Funded by SCOAP³.

1. Introduction

Despite being surpassingly successful, the Standard Model (SM) falls short of proffering a natural and well-founded rationale for the observed sub-eV neutrino masses. Diversely, the type-III see-saw model, one of the three UV completions of the so-called Weinberg operator [1] at the tree-level [2], based on the annexation of the SM by weak gauge triplet of fermion field [3] seems to explain the minuteness of neutrino masses readily. Though the see-saw anchors are naturally motivated to have very high scale masses, if balanced with appropriate Yukawa couplings, nothing precludes them from having mass at TeV scale, and thus a well-to-do phenomenology at the Large Hadron Collider (LHC). Phenomenological outcome of this model has been studied all-encompassingly in the literature [4–19]. At the LHC, a number of collider searches looking for the triplet fermions have been carried out [20–25], and the observations being consistent with the SM expectations, these searches have derived exclusion limits at 95% confidence level (CL) on the mass of the triplet fermions. Assuming only one generation

of them in the flavour-democratic scenario, the ATLAS collaboration has put the most stringent limit of 910 GeV by combining the recent multi-lepton search [25] with the already published dilepton search [24]. This limit extends to 1140 GeV when three mass-degenerate triplet fermions are assumed [18].¹

Not only are the signals for the leptonic final states considered in the abovementioned LHC searches [20–25] suppressed by the leptonic branching fractions of the SM bosons (W, Z, h), but they are also beset with considerably large SM backgrounds. Consequently, these searches are deemed not to be sensitive enough in probing the triplet fermions much heavier than 1 TeV. Moreover, these searches are not designed to reconstruct the triplet mass. This behoves us to look for complementary final states, such as multiple leptons and fat-jets resulting from the hadronically decaying SM bosons, which are not only clean and thus sensitive enough in probing the TeV scale triplets but also allow kinematic reconstruction of them. To this end, we perform a systematic and comprehensive search for the triplet fermions in final states with multiple leptons and fat-jets.

* Corresponding author.

E-mail addresses: saiyad.a@iopb.res.in (S. Ashanujjaman), kirti.gh@gmail.com (K. Ghosh).

¹ Three generations of triplet fermions are required to generate three non-vanishing neutrino masses. Note that one (two) generation(s) of them would not suffice to explain more than one (two) non-zero neutrino masses.

The rest of this work is structured as follows. In Section 2, we briefly discuss the productions and decays of the triplet fermions. We perform a systematic and comprehensive collider analysis for the triplet fermions in final states with multiple leptons and fat-jets at the 13 TeV LHC in Section 3 followed by a summary in Section 4.

2. The triplet fermions

The type-III see-saw model employs, in addition to the SM field content, three generations of right-handed $SU(2)_L$ triplet fermions with vanishing hypercharge

$$\Sigma = \begin{pmatrix} \Sigma_R^0/\sqrt{2} & \Sigma_R^+ \\ \Sigma_R^- & -\Sigma_R^0/\sqrt{2} \end{pmatrix};$$

and the relevant triplet Yukawa and mass terms are given by

$$-\mathcal{L} \supset \frac{1}{2} (M_\Sigma)_{ij} \text{Tr} \left(\bar{\Sigma}_i \Sigma_j \right) + \sqrt{2} (Y_\Sigma)_{i\alpha} \tilde{H}^\dagger \bar{\Sigma}_i L_\alpha + \text{h.c.},$$

where i, j and α are the generation indices which run over 1, 2 and 3, M_Σ is the Majorana mass matrix for Σ , $\tilde{\Sigma}$ denotes charge-conjugation of Σ , i.e. $\tilde{\Sigma} = C \bar{\Sigma}^T$ with C being the charge-conjugation matrix, Y_Σ is the Yukawa matrix, $L = (v_L, \ell_L)^T$ is the left-handed SM lepton doublet, and H is the SM Higgs doublet. For simplicity, we assume $M_\Sigma = m_\Sigma \mathbb{1}_{3 \times 3}$, i.e. all three generations of triplets are mass-degenerate. The above Lagrangian leads to the so-called *see-saw formula* for the light neutrinos: $m_\nu \approx -\frac{v^2}{2} Y_\Sigma^T M_\Sigma^{-1} Y_\Sigma$. For a given M_Σ , the well-known *Casas-Ibarra parametrisation* [26,27] enables one to find the most general texture of Y_Σ to reproduce the low-energy neutrino oscillation parameters [28] which we avert to discuss in this work, see [16–18].

The triplet fermions are pair produced copiously at the LHC by quark-antiquark annihilation via s -channel γ/Z and W^\pm exchanges

$$q\bar{q} \rightarrow W^* \rightarrow \Sigma^\pm \Sigma^0, \quad \text{and} \quad q\bar{q} \rightarrow \gamma^*/Z^* \rightarrow \Sigma^+ \Sigma^-.$$

They are also pair produced via photon-photon fusion processes²: $\gamma\gamma \rightarrow \Sigma^+ \Sigma^-$. Their production at the LHC has been widely studied in the literature [4–19]. In our analysis, we evaluate the leading order (LO) production cross-sections using the UFO modules generated from SARAH [29,30] in MadGraph [31,32] with the *LUXqed17-plus-PDF4LHC15-nnlo-100* parton distribution function [33–35]. The total LO pair production cross-sections varies from 585 fb to 0.02 fb for 400 GeV to 2 TeV triplet mass [4–19]. Following Ref. [36], we naively scale the LO cross-section by an overall K -factor of 1.30.³

After being produced, the triplet fermions undergo two types of decays – (i) the *heavy state transitions* due to the radiative mass-splitting of $\Delta m = m_{\Sigma^+} - m_{\Sigma^0} \sim 167$ MeV [37], and (ii) the *two-body decays* into a SM boson (W, Z, h) and a lepton (ℓ, ν). For the Yukawa couplings ($Y_\Sigma)_{i\alpha}$ not smaller than $\mathcal{O}(10^{-8})$, the later decay modes subjugate the former ones ensuring their prompt decays into two SM particles [16–18]. The relevant partial decay widths are given by

$$\Gamma(\Sigma_i^{0(\pm)} \rightarrow XY_\alpha^{(\prime)}) = \kappa \frac{m_\Sigma}{64\pi} |(Y_\Sigma)_{i\alpha}|^2 f \left(\frac{m_X}{m_\Sigma} \right),$$

² They are also pair produced via vector-boson fusion processes with one or two associated forward jets at the LHC. However, we do not consider these due to their small contribution.

³ Ref. [36] has reported the leading QCD corrections to the production of triplet fermions at hadron colliders. The resulting next-to-leading order (NLO) K -factors varies from 1.24 to 1.37 over a triplet mass range of 1 TeV to 2 TeV.

where $XY_\alpha \ni h\nu_\alpha, Z\nu_\alpha, W^\pm \ell_\alpha^\mp, XY'_\alpha \ni h\ell_\alpha^\pm, Z\ell_\alpha^\pm, W^\pm \nu_\alpha$, $f(r) = (1-r^2)^2(1+\kappa'r^2), \kappa(\kappa') = 1, 2(0, 2, 2)$ for $X = h, Z, W^\pm$, respectively. The branching fractions for the h, Z and W decay modes are, respectively, 25%, 25% and 50%. For simplicity, all three generations of triplets are assumed to be mass-degenerate.⁴ Further, we assume identical branching fractions across all lepton flavours (*flavour-democratic scenario*).⁵ This is readily achieved by choosing the triplet Yukawa couplings that are compatible with the existing constraints [38–40] as well as the neutrino oscillation data [28], see [16–18].

3. Collider phenomenology

At the LHC, the triplet fermions are pair produced aplenty followed by their prompt decays to a SM lepton (ℓ, ν) and a boson (W, Z, h) leading to multifarious final state signatures. The characteristic signature of TeV scale triplets⁶ would be vastly boosted final state lepton and boson which are likely to be largely separated in the azimuth plane. The jets stemming from the sufficiently highly boosted boson would be collimated. The hadronically decaying bosons, thus, are more likely to manifest as a single fat-jet rather than two resolved jets. In what follows, we perform a systematic and comprehensive collider study for the triplet fermions in the final states with multiple leptons and fat-jets. The processes contributing to the final state signatures of our interest are summarised in the following:

(i) *One lepton and fat-jets*: Both pair and associated production of charged triplets contribute to this final state:

- (a) $\Sigma^\pm \Sigma^\mp \rightarrow \ell^\pm Z/h\nu W^\mp \rightarrow \ell^\pm \nu J_{Z/h} J_W$,
- (b) $\Sigma^\pm \Sigma^- \rightarrow \nu W^+ \nu W^- \rightarrow \ell^\pm \nu \nu \nu J_W$,
- (c) $\Sigma^\pm \Sigma^0 \rightarrow \ell^\pm Z/h\nu Z/h \rightarrow \ell^\pm \nu J_{Z/h} J_{Z/h}$,
- (d) $\Sigma^\pm \Sigma^0 \rightarrow \nu W^\pm \ell^\pm W^\mp \rightarrow \ell^\pm \nu J_W J_W$,

where $J_{W/Z/h}$ denotes a fat-jet emanating from $W/Z/h$. For process (b), neutrinos result from both triplet fermions making kinematic reconstruction of the latter challenging. For all other processes, one of the triplets decays to ℓ^\pm and $W/Z/h$, where the latter manifests as $J_{W/Z/h}$. The triplets being in the TeV regime, ℓ^\pm and $J_{W/Z/h}$ are deemed to be largely separated in the azimuth plane. Therefore, m_Σ can be reconstructed from the invariant mass distribution of the lepton and the farthest $J_{ZW//h}$ in the azimuth plane.

(ii) *Same-sign dilepton and fat-jets*: Only the following process contributes to this final state:

$$\Sigma^\pm \Sigma^0 \rightarrow \ell^\pm Z/h\ell^\pm W^\mp \rightarrow \ell^\pm \ell^\pm J_{Z/h} J_W.$$

The invariant mass distribution of $J_{W/Z/h}$ and the farthest lepton in the azimuth plane would peak at m_Σ .

(iii) *Opposite-sign dilepton and fat-jets*: The processes contributing to this final states are as follows:

⁴ While, *a priori*, nothing precludes the mass from varying across the generations, including such a possibility only introduces additional parameters (and thus complications) without adding anything qualitatively different to the discussion.

⁵ We accentuate that the flavour democratic scenario does not necessarily be an *ad-hoc* assumption; rather, it could be a consequence of degenerate mass spectrum for both the light and heavy neutrinos or could be a repercussion of the information lost in integrating the heavy leptons out [18]. Also, this assumption facilitates an easy comparison with existing search paradigms adopted by the ATLAS/CMS collaborations. However, relaxation of this assumption may significantly alter the phenomenology, and thus the exclusion limit, see [18].

⁶ The recent ATLAS multi-lepton search [25] has already excluded triplet fermions with masses below 910 GeV assuming only one generation of them in the flavour-democratic scenario. This limit extends to 1140 GeV when three mass-degenerate triplets are considered [18].

Table 1The partonic level signal ($m_\Sigma = 1150$ GeV) cross-sections (in fb) for the different final states.

	One lepton	Same-sign dilepton	Opposite-sign dilepton	Trilepton + no jet	Trilepton + jets	Tetralepton
$\Sigma^+ \Sigma^-$	0.235	–	0.161	–	0.017	0.023
$\Sigma^\pm \Sigma^0$	0.408	0.101	0.101	0.025	0.107	0.018

- (a) $\Sigma^+ \Sigma^- \rightarrow \ell^+ Z/h \ell^- Z/h \rightarrow \ell^+ \ell^- J_{Z/h} J_{Z/h}$,
 (b) $\Sigma^\pm \Sigma^\mp \rightarrow \ell^\pm Z/h \nu W^\mp \rightarrow \ell^\pm \ell^\mp \nu \nu J_{Z/h}$,
 (c) $\Sigma^\pm \Sigma^0 \rightarrow \ell^\pm Z/h \ell^\mp W^\pm \rightarrow \ell^\pm \ell^\mp J_{Z/h} J_W$.

Similar to the above channel, the invariant mass distribution of $J_{W/Z/h}$ and the farthest lepton in the azimuth plane would yield m_Σ .

(iv) *Trilepton without fat-jet*: Both pair and associated production of charged triplets contribute to this final state:

- (a) $\Sigma^\pm \Sigma^0 \rightarrow \nu W^\pm \ell^\pm (\mp) W^{\mp(\pm)} \rightarrow \ell^\pm \ell^\mp \ell^\pm \nu \nu \nu$,
 (b) $\Sigma^\pm \Sigma^0 \rightarrow \nu W^\pm \nu Z/h \rightarrow \ell^\pm \ell^+ \ell^- \nu \nu$.

Here, both the triplets lead to a neutrino in the final state, making their kinematic reconstruction challenging.

(v) *Trilepton and one fat-jet*: Both pair and associated production of charged triplets contribute to this final state:

- (a) $\Sigma^\pm \Sigma^\mp \rightarrow \ell^\pm Z/h \nu W^\mp \rightarrow \ell^\pm \ell^+ \ell^- \nu J_W$,
 (b) $\Sigma^\pm \Sigma^0 \rightarrow \ell^\pm Z/h \nu Z/h \rightarrow \ell^\pm \ell^+ \ell^- \nu J_{Z/h}$,
 (c) $\Sigma^\pm \Sigma^0 \rightarrow \ell^\pm Z/h \ell^\pm (\mp) W^{\mp(\pm)} \rightarrow \ell^\pm \ell^\pm \ell^\mp \nu J_{Z/h}$.

For processes (a) and (b), Σ^\pm decays to ℓ^\pm and Z/h which further decays to $\ell^+ \ell^-$. For process (c), Σ^\pm decays to ℓ^\pm and $J_{Z/h}$. Therefore, for the events with an on-Z lepton pair,⁷ the peak of the invariant mass distribution of the trilepton system is expected to yield m_Σ , whereas, for those with no on-Z lepton pair, m_Σ can be reconstructed from the invariant mass distribution of $J_{Z/h}$ and the farthest lepton in the azimuth plane.

(vi) *Tetralepton with/without one fat-jet*: Both pair and associated production of charged triplets contribute to this final state:

- (a) $\Sigma^+ \Sigma^- \rightarrow \ell^+ Z/h \ell^- Z/h \rightarrow \ell^+ \ell^+ \ell^- \ell^- J_{Z/h}$.
 (b) $\Sigma^\pm \Sigma^\mp \rightarrow \ell^\pm Z/h \nu W^\mp \rightarrow \ell^\pm \ell^+ \ell^- \ell^\mp \nu \nu$.
 (c) $\Sigma^\pm \Sigma^0 \rightarrow \ell^\pm Z/h \ell^\pm (\mp) W^{\mp(\pm)} \rightarrow \ell^\pm \ell^\pm \ell^\mp \ell^\pm (\mp) J_W$.

All the events necessarily contain an on-Z lepton pair. The invariant mass distribution of the on-Z lepton pair and the farthest lepton between the ones which are not part of the on-Z lepton pair would peak at m_Σ .

Table 1 displays the partonic level cross-sections (in fb) for the different final states for the signal with $m_\Sigma = 1150$ GeV at the 13 TeV LHC. These numbers are a rough guide but suggest that a handful of signal events would be obtained at the LHC for all the final states discussed above. We next give a brief description of reconstruction and selection of various physics objects, classification of events into several mutually exclusive analysis channels and event selection.

3.1. Object reconstruction and selection

We use Delphes [41] to reconstruct different objects, namely photons, electrons, muons and jets. Constituents of the *would-be* fat-jets are clustered using the *anti-k_T* algorithm [42] with the

winner-take-all axis with the characteristic fat-jet radius $R = 0.8$ as implemented in FastJet [43]. We use the *jet pruning* algorithm [44,45], setting the parameters to their default values, *viz.* $z_{cut} = 0.1$ and $R_{cut} = 0.5$ [44], to remove the softer and wide-angle QCD emissions from the fat-jets. Further, an inclusive jet shape termed as *N-subjettiness*, τ_N , [46,47] is used to unfold the multi-prong nature of the fat-jets. We choose the *one-pass k_T-axes* for the minimization procedure, and take the thrust parameter $\beta = 1$. The reconstructed leptons (electrons and muons) and fat-jets are required to have transverse momentum $p_T > 10$ and 30 GeV, respectively, and they must lie within the tracking system acceptance, pseudorapidity $|\eta| < 2.5$. The relative isolation⁸ is required to be smaller than 12%(15%) for electrons (muons). Such stringent lepton isolation requirements significantly suppress the reducible backgrounds. The selected leptons and jets are ordered by decreasing p_T (ℓ_0, ℓ_1, \dots and J_0, J_1, \dots). Often, some of the jets are misidentified as leptons. Following the Ref. [48], we take the probability of 0.1–0.3% for a jet to be misidentified as a lepton. Furthermore, bremsstrahlung interactions of electrons with the inner detector material often lead to their charge misidentification. We adopt the charge misidentification probability from Ref. [49]: $P(p_T, \eta) = \sigma(p_T) \times f(\eta)$, where $\sigma(p_T)$ and $f(\eta)$ ranges from 0.02 to 0.1 and 0.03 to 1, respectively. Finally, the missing transverse momentum vector \vec{p}_T^{miss} (with magnitude p_T^{miss}) is estimated using all the reconstructed particle-flow objects in an event.

3.2. SM backgrounds

We next briefly mention the SM processes which could resemble the abovementioned final states. The relevant processes can be classified into two classes – reducible and irreducible backgrounds. The SM processes giving rise to one or more prompt leptons, such as Drell-Yan processes, VV ($V = W, Z/\gamma^*$), VVV , $VVVV$, $t\bar{t}$, $t\bar{t}V$, single top production (tb, tW, tj) and Higgs-strahlung ($Vh, VVh, t\bar{t}h$) processes, constitute the irreducible backgrounds in this analysis. On the contrary, the reducible backgrounds are from the SM processes like $Z/\gamma^* + \text{jets}$ and $t\bar{t} + \text{jets}$, where a jet is misidentified as lepton or additional leptons originate from heavy quark decays. The reducible backgrounds are significantly suppressed by applying stringent lepton isolation requirements. All the background samples are generated in association with up to two jets using MadGraph [31,32] at the LO using the 5 flavour scheme followed by MLM matching in PYTHIA [50]. The background samples are normalised at least to the NLO prediction [51–73].

3.3. Event selection

After object selection, we make our identification of the $W/Z/h$ -fat-jets, denoted as $J_{W/Z/h}$, satisfying the conditions⁹:

⁸ The relative isolation of a lepton is defined as the scalar p_T sum, normalized to the lepton p_T , of photons and hadrons within a cone of $\Delta R = 0.5$ around the lepton.

⁹ The *N-subjettiness*, τ_N , is a good measure of the number of subjets a jet is presumably composed of. The ratio τ_{N-1}/τ_{N-1} is, thus, an useful discriminant between the *N*- and (*N*–1)-prong jets. Being two-prong in nature, the jets emanating from the sufficiently highly boosted $W/Z/h$ -bosons tend to have lower $\tau_{21} = \frac{p_T}{\tau_1}$ as com-

⁷ An opposite-sign same flavour lepton pair with an invariant mass within the Z-boson mass window, *i.e.* $m_Z \pm 15$ GeV is termed as “on-Z lepton pair”.

Table 2

The preselection criteria for the considered analysis channels. All the selection cuts are in GeV. The symbol “–” means no requirement is made.

Selection criteria	<i>1L-1J</i>	<i>1L-2J</i>	<i>SSD-1J</i>	<i>OSD-1J</i>	<i>3L-0J</i>	<i>3L-1J</i>	<i>4L</i>
n_ℓ	= 1	= 1	= 2	= 2	= 3	= 3	= 4
$ \sum Q_\ell $	= 1	= 1	= 2	= 0	–	–	–
$n_{J_{W/Z/h}}$	= 1	= 2	≥ 1	≥ 1	= 0	= 1	≥ 0
$p_T(\ell_0)$	> 200	> 200	> 400	> 400	> 300	> 300	> 400
$p_T(\ell_1)$	–	–	> 100	> 100	> 100	> 100	> 200
p_T^{miss}	> 100	> 100	–	–	> 100	–	–
Low $m_{\ell\ell}^{\text{OSSF}}$ veto	–	–	> 12	> 12	> 12	> 12	> 12
Z-veto	–	–	Yes	Yes	–	–	–

$$m(J) \in [70, 140] \text{ GeV}, p_T(J) > 200 \text{ GeV} \text{ and } \tau_{21} < 0.7.$$

Based on the number of leptons and $J_{W/Z/h}$ (n_ℓ and $n_{J_{W/Z/h}}$) and the absolute value of the sum of charges of the leptons ($|\sum Q_\ell|$), the events are categorised into seven distinct final states — *1L-1J*, *1L-2J*, *SSD-1J*, *OSD-1J*, *3L-0J*, *3L-1J* and *4L* (see Table 2), while the events not falling under these channels are thrown away. As mentioned earlier, the leptons and bosons coming from the decays of the TeV scale triplets would carry sufficiently high momenta that stronger cuts on the leptons' p_T and/or p_T^{miss} would be utile in curtailing the SM background while keeping the signal all but unharmed. The event selection proceeds in two steps: the preselection and the channel-specific event selection. The preselection requirements are primarily based on $p_T(\ell_0)$, $p_T(\ell_1)$ and p_T^{miss} , see Table 2. Events containing an opposite-sign same-flavour (OSSF) lepton pair with invariant mass below 12 GeV are thrown away in all the channels to reduce background contributions from low-mass resonances. Furthermore, to suppress the overwhelming background contributions from the Drell-Yan processes in the *SSD-1J* and *OSD-2J* channels, events containing an opposite-sign same-flavour lepton pair with an invariant mass within the nominal Z-boson mass window, *i.e.* $m_Z \pm 15$ GeV are vetoed.¹⁰

We next briefly discuss the channel-specific selection criteria, which appreciably reduce the remaining SM backgrounds without impinging much on the signal strength. We use various kinematic distributions as guiding premises to choose the appropriate selection cuts.

We display different normalised kinematic distributions for the *1L-1J* events in Fig. 1 for a benchmark point: $m_\Sigma = 1150$ GeV. In the top panel, we show the $p_T(\ell_0)$ (left) and p_T^{miss} (right) distributions. The middle panel displays the H_T (left) and $m_{\text{eff}} = L_T + H_T + p_T^{\text{miss}}$ (right) distributions, where $L_T(H_T)$ is the scalar sum of all the leptons' (jets') p_T . In the bottom panel, the left plot shows the distribution of the azimuthal separation between ℓ_0 and p_T^{miss} , $|\Delta\phi(\ell_0, p_T^{\text{miss}})|$, whereas the right plot shows the $p_T(J_0)$ distribution. As expected, the kinematic distributions for the signal are much harder than those for the background, see Fig. 1. Consequently, harder cuts on these kinematic variables are expected to suppress the remaining background without impinging much on the signal strength. On the other hand, $|\Delta\phi(\ell_0, p_T^{\text{miss}})|$ turns out to be efficient in discriminating the background (in particular, the background from single W-boson) and signal. We impose the following selection cuts:

$$\mathbf{SI-1:} p_T(\ell_0) > 400 \text{ GeV} \text{ and } p_T^{\text{miss}} > 400 \text{ GeV},$$

pared to the overwhelming one-prong QCD or top jets. The cut on τ_{21} significantly suppresses the background contributions from the QCD or top-jets.

¹⁰ Note that, in order to reduce the contributions originating from electron charge misidentification, the Z-veto is also applied to the *SSD-1J* events.

$$\mathbf{SI-2:} H_T > 500 \text{ GeV}, m_{\text{eff}} > 1800 \text{ GeV} \text{ and}$$

$$p_T(J_0) > 300 \text{ GeV},$$

$$\mathbf{SI-3:} |\Delta\phi(\ell_0, p_T^{\text{miss}})| > 0.5.$$

Also displayed, in Fig. 2, is the normalised distribution of $\tau_{21}(J_0)$ for the *1L-1J* events passing the *S1-1*, *S1-2* and *S1-3* cuts. As expected, an inordinately large fraction of the signal events has lower τ_{21} as compared to the remaining background events. Therefore, to further improve the signal-to-background ratio, we impose the following selection cut:

$$\mathbf{SI-4:} \tau_{21}(J_0) < 0.5.$$

We display the effect of the selection cuts on the signal and background strengths for the *1L-1J* channel in Table 3. It shows the progression of the number of expected background and signal ($m_\Sigma = 1150$ GeV) events as the subsequent selection cuts are imposed for 1000 fb^{-1} luminosity at the 13 TeV LHC. As we expected, the preselection cuts and channel-specific selection cuts effectively vanquish the SM backgrounds while keeping a large fraction of the signal.

As for the other channels, the distributions (and, hence, the discussions) are very similar, and for brevity's sake, we do not discuss these in detail, instead summarise all the channel specific selection cuts in Table 4. The variable L_T (shown in Fig. 3) along with the others like H_T , m_{eff} and $p_T(J_0)$ turn out to be very useful in suppressing the SM background over the signal for all the channels. Table 4 also shows the number of expected background and signal ($m_\Sigma = 1150$ GeV) events after all the selection cuts are imposed for 1000 fb^{-1} luminosity at the 13 TeV LHC.

In order to enhance the sensitivity of this search, the selected events in each channel are divided into several independent search bins using a primary kinematic discriminant between the signal and background. The discriminants used in different channels are as follows:

- **1L-1J:** the invariant mass of the lepton and the fat-jet: $m_{\ell J} = m_{\ell_0 J_0}$;

- **1L-2J:** the invariant mass of the lepton and the farthest fat-jet in the azimuth plane:

$$m_{\ell J} = m_{\ell_0 J_0} \text{ if } \Delta\phi(\ell_0, J_0) > \Delta\phi(\ell_0, J_1)$$

$$= m_{\ell_1 J_1} \text{ otherwise;}$$

- **SSD-1J and OSD-1J:** (i) for events with exactly one $J_{W/Z/h}$: the invariant mass of the fat-jet and the farthest lepton in the azimuth plane:

$$m_{\ell J} = m_{\ell_0 J_0} \text{ if } \Delta\phi(\ell_0, J_0) > \Delta\phi(\ell_1, J_0)$$

$$= m_{\ell_1 J_0} \text{ otherwise;}$$

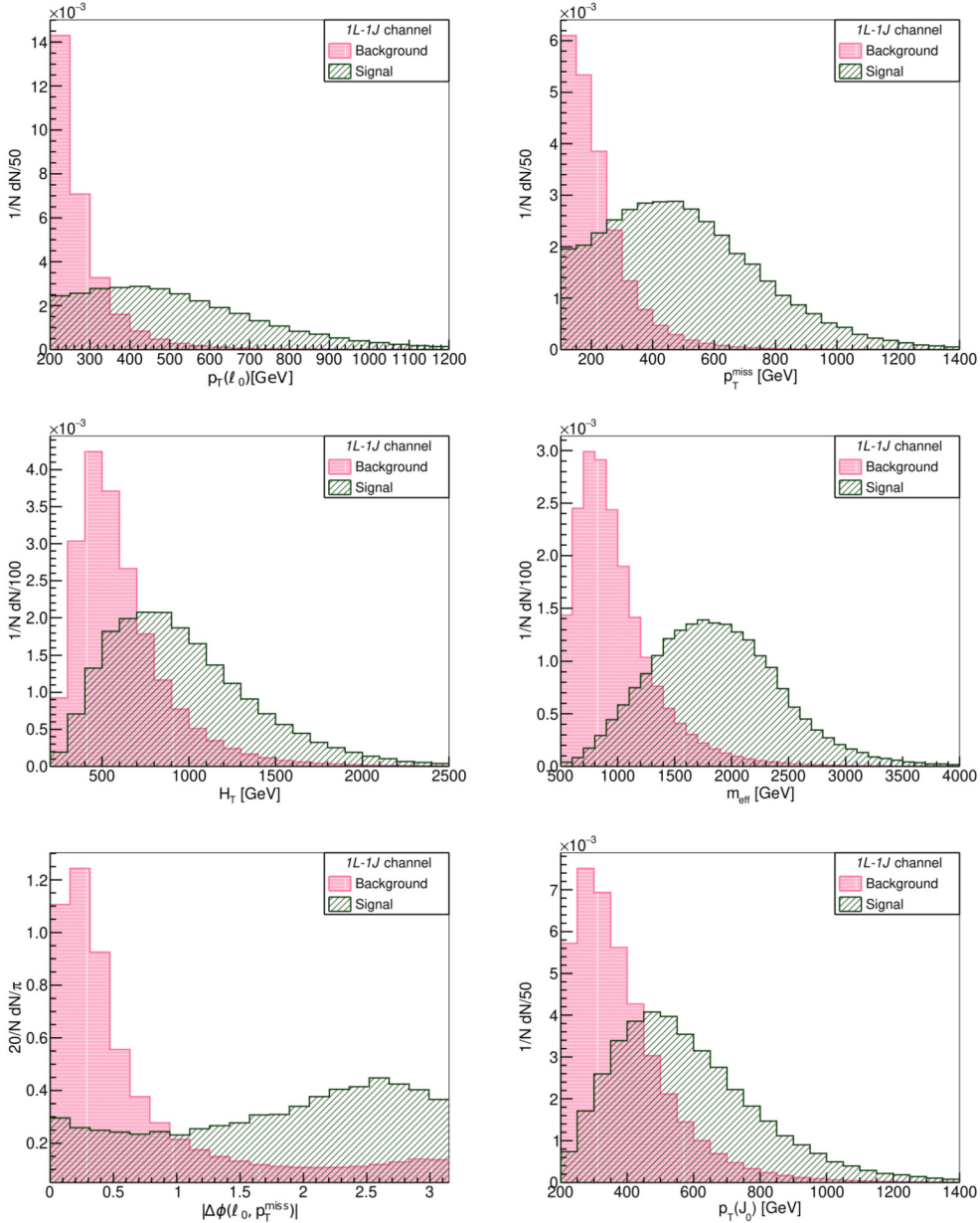


Fig. 1. Normalised kinematic distributions for signal ($m_\Sigma = 1150$ GeV) and background in the 1L-1J channel. Top panel: lepton p_T (left) and p_T^{miss} (right); middle panel: H_T (left) and m_{eff} (right); bottom panel: $\Delta\phi(\ell_0, p_T^{\text{miss}})$ (left) and $W/Z/h$ -fat-jet p_T (right).

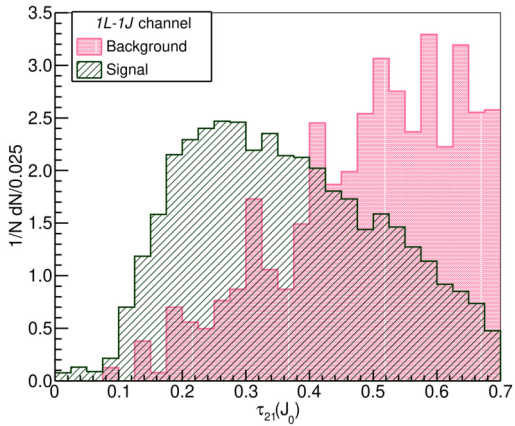


Fig. 2. Normalised distribution of $\tau_{21}(J_0)$ after passing the S1-1, S1-2 and S1-3 cuts for signal ($m_\Sigma = 1150$ GeV) and background in the 1L-1J channel.

(ii) for events with more than one $J_{W/Z/h}$:

$$m_{\ell J} = m_{\ell_0 J_0} \text{ if } |m_{\ell_0 J_0} - m_{\ell_1 J_1}| < |m_{\ell_0 J_1} - m_{\ell_1 J_0}| \\ = m_{\ell_0 J_1} \text{ otherwise;}$$

- **3L-QJ:** Missing neutrinos do not allow kinematic reconstruction of the triplets in this channel, and, thus, we use $L_T + p_T^{\text{miss}}$ as primary kinematic discriminant;
- **3L-1J:** (i) for events with one on-Z lepton pair, the invariant mass of the trilepton system: $m_{\ell_0 \ell_1 \ell_2}$; (ii) for events with no on-Z lepton pair: the invariant mass of the fat-jet and the farthest lepton in the azimuth plane;
- **4L:** the invariant mass of the on-Z lepton pair and the farthest lepton in the azimuth plane: $m_{(\ell\ell)Z\ell}$.

For all the channels except the 3L-QJ one, the distribution of the primary discriminant peaks at the triplet mass and thus could be used to reconstruct the same. We summarise the binning scheme

Table 3

The number of expected background and signal ($m_{\Sigma} = 1150$ GeV) events in the $1L-1J$ channel after passing various cuts for 1000 fb^{-1} luminosity at the 13 TeV LHC.

1L-1J channel					
Event sample	Preselection	SI-1	SI-2	SI-3	SI-4
Drell-Yan	$\sim 2.9 \times 10^5$	5119	4057	221	98
$t\bar{t}$	$\sim 1.7 \times 10^5$	291	190	44	20
Other backgrounds	$\sim 1.7 \times 10^4$	239	185	25	14
Total background	$\sim 4.8 \times 10^5$	5649	4432	290	132
Signal	330	126	93	90	71

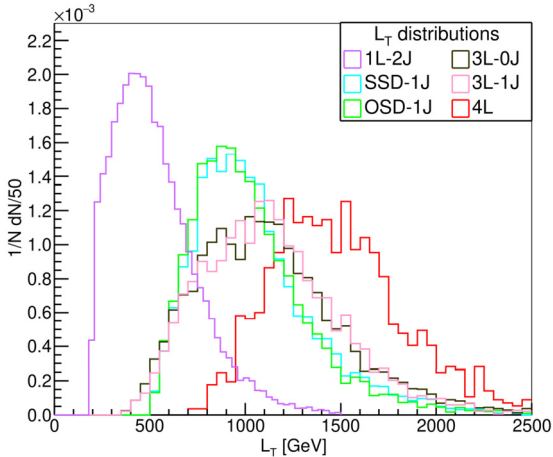


Fig. 3. Normalised distribution of L_T for the signal ($m_{\Sigma} = 1150$ GeV) in different channels.

Table 4

Summary of the channel-specific selection cuts along with the number of expected background and signal ($m_{\Sigma} = 1150$ GeV) events after all the selection cuts are imposed for 1000 fb^{-1} luminosity at the 13 TeV LHC. All the dimensionful cuts are in GeV.

Channel	Selection cuts	Background	Signal
1L-2J	$p_T(\ell_0) > 400, p_T^{\text{miss}} > 300, \Delta\phi(\ell_0, p_T^{\text{miss}}) > 0.5$	74	63
SSD-1J	$L_T > 600, H_T > 500, m_{\text{eff}} > 1600, p_T(J_0) > 300$	81	32
OSD-1J	$L_T > 700, H_T > 500, m_{\text{eff}} > 2000, p_T(J_0) > 400, \tau_{21}(J_0) < 0.6$	131	46
3L-0J	$L_T > 600, m_{\text{eff}} > 1500, L_T/H_T > 1.0, p_T^{\text{miss}}/H_T > 0.4$	67	24
3L-1J	$L_T > 700, m_{\text{eff}} > 1600, p_T(J_0) > 300, L_T/H_T > 1.0$	28	20
4L	$L_T > 1000, m_{\text{eff}} > 1600$	9	8

in Table 5, which yields a total of 50 statistically independent search bins. The width of the bins is chosen to ensure smooth behaviour for the expected background and signal distributions. The underflow (overflow) events are contained in the first (last) bin for each channel.

Fig. 4 displays the distributions of the primary kinematic discriminants for the signal ($m_{\Sigma} = 1150$ GeV) and background events for all the channels. The events are weighted for 1000 fb^{-1} luminosity at the 13 TeV LHC. As expected, these distributions (except the one for 3L-0J channel) peak in 1000–1200 GeV bin, and thereby reconstructing the triplet mass; a simple rebinning of these distributions with smaller bin widths would make this mass reconstruction apparent.

Table 5

Binning scheme of different channels.

Channel	Kinematic discriminant	Range (GeV)	Number of bins
1L-1J	$m_{\ell_0 J_0}$	[600, 2000]	7
1L-2J	$m_{\ell_0 J_0}$ or $m_{\ell_1 J_1}$	[600, 2000]	7
SSD-1J	$m_{\ell_0 J_0}$ or $m_{\ell_1 J_0}$	[600, 2000]	7
OSD-1J	$m_{\ell_0 J_0}$ or $m_{\ell_1 J_0}$	[600, 2000]	7
3L-0J	$L_T + p_T^{\text{miss}}$	[750, 2750]	8
3L-1J	$m_{\ell_0 J_0}$ or $m_{\ell_1 J_0}$ or $m_{\ell_0 \ell_1 \ell_2}$	[600, 2000]	7
4L	$m_{(\ell\ell)_Z \ell}$	[600, 2000]	7

3.4. Discovery reach

We next estimate the discovery reach of the present search for the triplet fermions. To this end, we use a hypothesis tester named *Profile Likelihood Number Counting Combination* which uses the library *RooFit* [74] in the *ROOT* [75] environment. This hypothesis tester considers all the search bins as independent number counting channels with uncorrelated systematic errors. The uncertainties are included via the *Profile Likelihood Ratio*. For the sake of simplicity, we assume an overall 20% total uncertainty on the estimated background. Further, to avoid spurious exclusions/discoveries and to ensure robustness in statistical interpretations, we replace the less than one per-bin expected background yield at 3000 fb^{-1} with one background yield. This renders our estimated significances to be a bit conservative. In Fig. 5, we project the required luminosities for 3σ discovery of the triplet fermions in different analysis channels as a function of their mass; for brevity, we display the same for the most promising channels only. We see that the 1L-2J channel is the most promising one with the discovery reach of 1480 GeV, while the rest of the channels have a similar discovery reach of 1330–1350 GeV.¹¹

Since all the analysis channels considered in this search are mutually exclusive, it is reasonable to combine them. For the combined channels, we project the required luminosities for both 3σ and 5σ discoveries of the triplet fermions as a function of their mass in Fig. 6. The 5σ (3σ) discovery reach of this search is about 1265 (1380) and 1480 (1600) GeV, respectively, at 500 and 3000 fb^{-1} luminosities.

4. Summary

The CMS and ATLAS collaborations have performed several searches targeting the triplet fermions in the type-III see-saw model. However, the final states considered in these searches being beset with considerably large SM backgrounds are deemed not sensitive enough to probe the triplet fermions much heavier than 1 TeV. To this end, we perform a search for the triplet fermions in final states with multiple leptons and fat-jets that are cleaner than the usual LHC searches and allow reconstruction of the triplet mass. After performing a systematic and comprehensive search with seven distinct analysis channels, we project the required luminosities for both 3σ and 5σ discoveries of the triplet fermions as a function of their mass. The triplet fermions with mass as large

¹¹ Note that the 1L-channels are not suppressed by the leptonic branching fractions of the SM bosons, and thus, yield a sufficient number of signal events even for larger triplet mass. Moreover, not only does the requirement of two $J_{W/Z,h}$ in the final state vanquish the background, but it also allows kinematic reconstruction of the triplets without any ambiguity (see the top panel in Fig. 4). On the contrary, final states with higher lepton multiplicity (three or more) being suppressed by the leptonic branching fractions of the SM bosons are less sensitive in probing triplets with higher masses. Note that the recent CMS/ATLAS searches [20–25] targeting the triplet fermions in the type-III see-saw model rely on multi-lepton final states only, and thus, are not sensitive enough in probing them with higher masses.

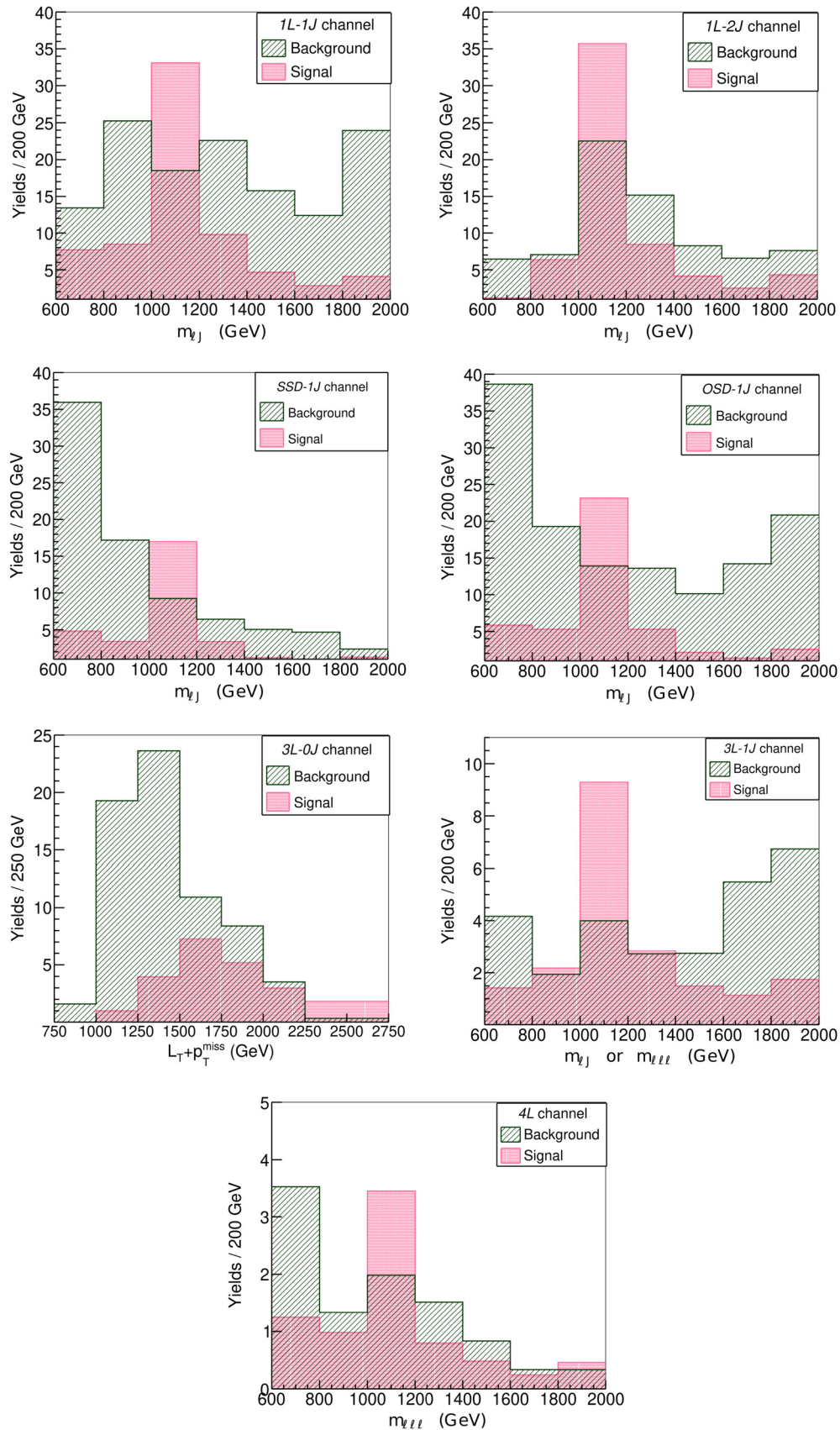


Fig. 4. Distributions of the primary kinematic discriminants for the signal ($m_\Sigma = 1150$ GeV) and background. The events are weighted for 1000 fb^{-1} luminosity at the 13 TeV LHC.

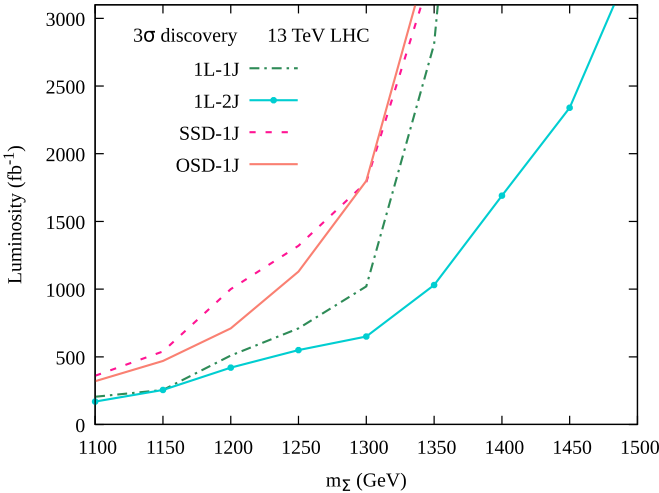


Fig. 5. Required Luminosity for 3σ discovery of the triplet fermions in different analysis channels.

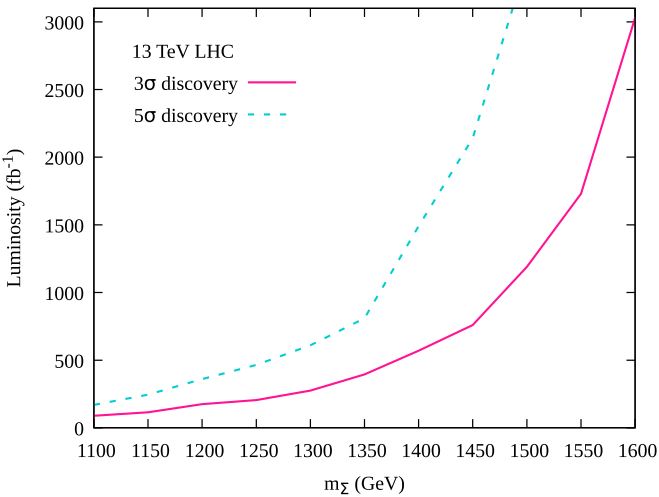


Fig. 6. Required Luminosity for 3σ and 5σ discovery of the triplet fermions in the combined channels.

as 1265 (1380) and 1480 (1600) GeV could be discovered with 5σ (3σ) significance at 500 and 3000 fb⁻¹ luminosities, respectively.¹² In closing, we mention that a search similar to the one presented in this work is prophesied to carry through for a large class of neutrino mass models containing new weak gauge multiplets. We undertake a detailed analysis for the same in a future work [76].

Declaration of competing interest

The authors declare that they have no known competing financial interests or personal relationships that could have appeared to influence the work reported in this paper.

¹² Though single production of the triplet fermions, in principle, in association with a SM lepton is possible, such processes are extremely suppressed both at pp and e^-e^+ colliders on account of their small mixing with the SM leptons. In view of pair production of the triplet fermions, in the most optimistic scenario, a high energy e^-e^+ collider could probe them very close to its kinematic reach [13,15], i.e. 1500 GeV for a 3 TeV collider. Note that the 3σ (5σ) reach of our search at 3000 fb⁻¹ luminosity extends beyond (very close to) the kinematic reach of a 3 TeV e^-e^+ collider.

Acknowledgements

KG acknowledges support from the DST INSPIRE Research Grant [DST/INSPIRE/04/2014/002158] and SERB Core Research Grant [CRG/2019/006831]. The simulations were supported in part by the SAMKHYA: High Performance Computing Facility provided by Institute of Physics, Bhubaneswar.

References

- [1] S. Weinberg, Baryon and lepton nonconserving processes, *Phys. Rev. Lett.* **43** (1979) 1566–1570.
- [2] E. Ma, Pathways to naturally small neutrino masses, *Phys. Rev. Lett.* **81** (1998) 1171–1174, arXiv:hep-ph/9805219.
- [3] R. Foot, H. Lew, X.G. He, G.C. Joshi, Seesaw neutrino masses induced by a triplet of leptons, *Z. Phys. C* **44** (1989) 441.
- [4] B. Bajc, G. Senjanovic, Seesaw at LHC, *J. High Energy Phys.* **08** (2007) 014, arXiv: hep-ph/0612029.
- [5] P. Fileviez Perez, Renormalizable adjoint SU(5), *Phys. Lett. B* **654** (2007) 189–193, arXiv:hep-ph/0702287.
- [6] P. Fileviez Perez, Supersymmetric adjoint SU(5), *Phys. Rev. D* **76** (2007) 071701, arXiv:0705.3589.
- [7] F. del Aguila, J.A. Aguilar-Saavedra, Electroweak scale seesaw and heavy Dirac neutrino signals at LHC, *Phys. Lett. B* **672** (2009) 158–165, arXiv:0809.2096.
- [8] F. del Aguila, J.A. Aguilar-Saavedra, Distinguishing seesaw models at LHC with multi-lepton signals, *Nucl. Phys. B* **813** (2009) 22–90, arXiv:0808.2468.
- [9] R. Franchescini, T. Hambye, A. Strumia, Type-III see-saw at LHC, *Phys. Rev. D* **78** (2008) 033002, arXiv:0805.1613.
- [10] A. Arhrib, B. Bajc, D.K. Ghosh, T. Han, G.Y. Huang, I. Puljak, G. Senjanovic, Collider signatures for heavy lepton triplet in type I+III seesaw, *Phys. Rev. D* **82** (2010) 053004, arXiv:0904.2390.
- [11] P. Bandyopadhyay, S. Choi, E.J. Chun, K. Min, Probing Higgs bosons via the type III seesaw mechanism at the LHC, *Phys. Rev. D* **85** (2012) 073013, arXiv:1112.3080.
- [12] C. Biggio, F. Bonnet, Implementation of the type III seesaw model in FeynRules/MadGraph and prospects for discovery with early LHC data, *Eur. Phys. J. C* **72** (2012) 1899, arXiv:1107.3463.
- [13] D. Goswami, P. Poulose, Direct searches of type III seesaw triplet fermions at high energy e^+e^- collider, *Eur. Phys. J. C* **78** (1) (2018) 42, arXiv:1702.07215.
- [14] Y. Cai, T. Han, T. Li, R. Ruiz, Lepton number violation: seesaw models and their collider tests, *Front. Phys.* **6** (2018) 40, arXiv:1711.02180.
- [15] A. Das, S. Mandal, T. Modak, Testing triplet fermions at the electron-positron and electron-proton colliders using fat jet signatures, *Phys. Rev. D* **102** (3) (2020) 033001, arXiv:2005.02267.
- [16] S. Jana, N. Okada, D. Raut, Displaced vertex and disappearing track signatures in type-III seesaw, arXiv:1911.09037.
- [17] A. Das, S. Mandal, Bounds on the triplet fermions in type-III seesaw and implications for collider searches, *Nucl. Phys. B* **966** (2021) 115374, arXiv:2006.04123.
- [18] S. Ashanujjaman, K. Ghosh, Type-III see-saw: phenomenological implications of the information lost in decoupling from high-energy to low-energy, *Phys. Lett. B* **819** (2021) 136403, arXiv:2102.09536.
- [19] C. Sen, P. Bandyopadhyay, S. Dutta, A. KT, Displaced Higgs production in type-III seesaw at the LHC/FCC, MATHUSLA and muon collider, arXiv:2107.12442.
- [20] ATLAS collaboration, Search for type-III seesaw heavy leptons in pp collisions at $\sqrt{s} = 8$ TeV with the ATLAS detector, *Phys. Rev. D* **92** (3) (2015) 032001, arXiv:1506.01839.
- [21] CMS collaboration, Search for evidence of the type-III seesaw mechanism in multilepton final states in proton-proton collisions at $\sqrt{s} = 13$ TeV, *Phys. Rev. Lett.* **119** (22) (2017) 221802, arXiv:1708.07962.
- [22] ATLAS collaboration, Search for type-III seesaw heavy leptons in proton-proton collisions at $\sqrt{s} = 13$ TeV with the ATLAS detector, ATLAS-CONF-2018-020.
- [23] CMS collaboration, Search for physics beyond the standard model in multilepton final states in proton-proton collisions at $\sqrt{s} = 13$ TeV, *J. High Energy Phys.* **03** (2020) 051, arXiv:1911.04968.
- [24] ATLAS collaboration, Search for type-III seesaw heavy leptons in dilepton final states in pp collisions at $\sqrt{s} = 13$ TeV with the ATLAS detector, *Eur. Phys. J. C* **81** (3) (2021) 218, arXiv:2008.07949.
- [25] ATLAS collaboration, Search for type-III seesaw heavy leptons in leptonic final states in pp collisions at $\sqrt{s} = 13$ TeV with the ATLAS detector, ATLAS-CONF-2021-023.
- [26] J.A. Casas, A. Ibarra, Oscillating neutrinos and $\mu \rightarrow e, \gamma$, *Nucl. Phys. B* **618** (2001) 171–204, arXiv:hep-ph/0103065.
- [27] A. Ibarra, G.G. Ross, Neutrino phenomenology: the case of two right-handed neutrinos, *Phys. Lett. B* **591** (2004) 285–296, arXiv:hep-ph/0312138.
- [28] I. Esteban, M.C. Gonzalez-Garcia, A. Hernandez-Cabreudo, M. Maltoni, T. Schwetz, Global analysis of three-flavour neutrino oscillations: synergies and tensions in the determination of θ_{23} , δ_{CP} , and the mass ordering, *J. High Energy Phys.* **01** (2019) 106, arXiv:1811.05487.

- [29] F. Staub, SARAH 4: a tool for (not only SUSY) model builders, *Comput. Phys. Commun.* 185 (2014) 1773–1790, arXiv:1309.7223.
- [30] F. Staub, Exploring new models in all detail with SARAH, *Adv. High Energy Phys.* 2015 (2015) 840780, arXiv:1503.04200.
- [31] J. Alwall, M. Herquet, F. Maltoni, O. Mattelaer, T. Stelzer, MadGraph 5: going beyond, *J. High Energy Phys.* 06 (2011) 128, arXiv:1106.0522.
- [32] J. Alwall, R. Frederix, S. Frixione, V. Hirschi, F. Maltoni, O. Mattelaer, H.S. Shaw, T. Stelzer, P. Torrielli, M. Zaro, The automated computation of tree-level and next-to-leading order differential cross sections, and their matching to parton shower simulations, *J. High Energy Phys.* 07 (2014) 079, arXiv:1405.0301.
- [33] A. Manohar, P. Nason, G.P. Salam, G. Zanderighi, How bright is the proton? A precise determination of the photon parton distribution function, *Phys. Rev. Lett.* 117 (24) (2016) 242002, arXiv:1607.04266.
- [34] A.V. Manohar, P. Nason, G.P. Salam, G. Zanderighi, The photon content of the proton, *J. High Energy Phys.* 12 (2017) 046, arXiv:1708.01256.
- [35] J. Butterworth, S. Carrazza, A. Cooper-Sarkar, A. De Roeck, J. Feltesse, S. Forte, J. Gao, S. Glazov, J. Huston, Z. Kassabov, et al., PDF4LHC recommendations for LHC Run II, *J. Phys. G* 43 (2016) 023001, arXiv:1510.03865.
- [36] R. Ruiz, QCD corrections to pair production of type III seesaw leptons at hadron colliders, *J. High Energy Phys.* 12 (2015) 165, arXiv:1509.05416.
- [37] M. Cirelli, N. Fornengo, A. Strumia, Minimal dark matter, *Nucl. Phys. B* 753 (2006) 178–194, arXiv:hep-ph/0512090.
- [38] A. Abada, C. Biggio, F. Bonnet, M.B. Gavela, T. Hambye, $\mu \rightarrow e\gamma$ and $\tau \rightarrow \ell\gamma$ decays in the fermion triplet seesaw model, *Phys. Rev. D* 78 (2008) 033007, arXiv:0803.0481.
- [39] S. Goswami, K.N. Vishnudath, N. Khan, Constraining the minimal type-III seesaw model with naturalness, lepton flavor violation, and electroweak vacuum stability, *Phys. Rev. D* 99 (7) (2019) 075012, arXiv:1810.11687.
- [40] C. Biggio, E. Fernandez-Martinez, M. Filaci, J. Hernandez-Garcia, J. Lopez-Pavon, Global bounds on the type-III seesaw, *J. High Energy Phys.* 05 (2020) 022, arXiv:1911.11790.
- [41] J. de Favereau, et al., DELPHES 3, a modular framework for fast simulation of a generic collider experiment, *J. High Energy Phys.* 02 (2014) 057, arXiv:1307.6346.
- [42] M. Cacciari, G.P. Salam, G. Soyez, The anti- k_t jet clustering algorithm, *J. High Energy Phys.* 04 (2008) 063, arXiv:0802.1189.
- [43] M. Cacciari, G.P. Salam, G. Soyez, Fastjet user manual, *Eur. Phys. J. C* 72 (2012) 1896, arXiv:1111.6097.
- [44] S.D. Ellis, C.K. Vermilion, J.R. Walsh, Techniques for improved heavy particle searches with jet substructure, *Phys. Rev. D* 80 (2009) 051501, arXiv:0903.5081.
- [45] S.D. Ellis, C.K. Vermilion, J.R. Walsh, Recombination algorithms and jet substructure: pruning as a tool for heavy particle searches, *Phys. Rev. D* 81 (2010) 094023, arXiv:0912.0033.
- [46] J. Thaler, K. Van Tilburg, Identifying boosted objects with N-subjettiness, *J. High Energy Phys.* 03 (2011) 015, arXiv:1011.2268.
- [47] J. Thaler, K. Van Tilburg, Maximizing boosted top identification by minimizing N-subjettiness, *J. High Energy Phys.* 02 (2012) 093, arXiv:1108.2701.
- [48] ATLAS collaboration, Electron efficiency measurements with the ATLAS detector using the 2015 LHC proton-proton collision data, ATLAS-CONF-2016-024.
- [49] ATLAS collaboration, Search for doubly charged Higgs boson production in multi-lepton final states with the ATLAS detector using proton-proton collisions at $\sqrt{s} = 13$ TeV, *Eur. Phys. J. C* 78 (3) (2018) 199, arXiv:1710.09748.
- [50] T. Sjöstrand, S. Ask, J.R. Christiansen, R. Corke, N. Desai, P. Ilten, S. Mrenna, S. Prestel, C.O. Rasmussen, P.Z. Skands, An introduction to PYTHIA 8.2, *Comput. Phys. Commun.* 191 (2015) 159–177, arXiv:1410.3012.
- [51] J.M. Campbell, R.K. Ellis, An update on vector boson pair production at hadron colliders, *Phys. Rev. D* 60 (1999) 113006, arXiv:hep-ph/9905386.
- [52] M.L. Ciccolini, S. Dittmaier, M. Kramer, Electroweak radiative corrections to associated VH and ZH production at hadron colliders, *Phys. Rev. D* 68 (2003) 073003, arXiv:hep-ph/0306234.
- [53] O. Brein, A. Djouadi, R. Harlander, NNLO QCD corrections to the Higgs-strahlung processes at hadron colliders, *Phys. Lett. B* 579 (2004) 149–156, arXiv:hep-ph/0307206.
- [54] S. Catani, M. Grazzini, An NNLO subtraction formalism in hadron collisions and its application to Higgs boson production at the LHC, *Phys. Rev. Lett.* 98 (2007) 222002, arXiv:hep-ph/0703012.
- [55] F. Campanario, V. Hankele, C. Oleari, S. Prestel, D. Zeppenfeld, QCD corrections to charged triple vector boson production with leptonic decay, *Phys. Rev. D* 78 (2008) 094012, arXiv:0809.0790.
- [56] G. Ballossini, G. Montagna, C.M. Carloni Calame, M. Moretti, O. Nicrosini, F. Piccinini, M. Treccani, A. Vicini, Combination of electroweak and QCD corrections to single W production at the Fermilab Tevatron and the CERN LHC, *J. High Energy Phys.* 01 (2010) 013, arXiv:0907.0276.
- [57] A. Bredenstein, A. Denner, S. Dittmaier, S. Pozzorini, NLO QCD corrections to $pp \rightarrow t\bar{t}b\bar{b} + X$ at the LHC, *Phys. Rev. Lett.* 103 (2009) 012002, arXiv:0905.0110.
- [58] S. Catani, L. Cieri, G. Ferrera, D. de Florian, M. Grazzini, Vector boson production at hadron colliders: a fully exclusive QCD calculation at NNLO, *Phys. Rev. Lett.* 103 (2009) 082001, arXiv:0903.2120.
- [59] N. Kidonakis, Two-loop soft anomalous dimensions for single top quark associated production with a W^- or H^- , *Phys. Rev. D* 82 (2010) 054018, arXiv:1005.4451.
- [60] J.M. Campbell, R.K. Ellis, C. Williams, Vector boson pair production at the LHC, *J. High Energy Phys.* 07 (2011) 018, arXiv:1105.0020.
- [61] O. Brein, R. Harlander, M. Wiesemann, T. Zirke, Top-quark mediated effects in hadronic Higgs-Strahlung, *Eur. Phys. J. C* 72 (2012) 1868, arXiv:1111.0761.
- [62] G. Bevilacqua, M. Worek, Constraining BSM physics at the LHC: four top final states with NLO accuracy in perturbative QCD, *J. High Energy Phys.* 07 (2012) 111, arXiv:1206.3064.
- [63] M.V. Garzelli, A. Kardos, C.G. Papadopoulos, Z. Trocsanyi, $t\bar{t}W^{+-}$ and $t\bar{t}Z$ hadroproduction at NLO accuracy in QCD with parton shower and hadronization effects, *J. High Energy Phys.* 11 (2012) 056, arXiv:1208.2665.
- [64] O. Brein, R.V. Harlander, T.J.E. Zirke, vh@nnlo - Higgs Strahlung at hadron colliders, *Comput. Phys. Commun.* 184 (2013) 998–1003, arXiv:1210.5347.
- [65] L. Altenkamp, S. Dittmaier, R.V. Harlander, H. Rzezhak, T.J.E. Zirke, Gluon-induced Higgs-strahlung at next-to-leading order QCD, *J. High Energy Phys.* 02 (2013) 078, arXiv:1211.5015.
- [66] D.T. Nhung, L. Ninh, M.M. Weber, NLO corrections to WWZ production at the LHC, *J. High Energy Phys.* 12 (2013) 096, arXiv:1307.7403.
- [67] N. Kidonakis, Top quark production, arXiv:1311.0283.
- [68] A. Denner, S. Dittmaier, S. Kallweit, A. Mück, HAWK 2.0: a Monte Carlo program for Higgs production in vector-boson fusion and Higgs strahlung at hadron colliders, *Comput. Phys. Commun.* 195 (2015) 161–171, arXiv:1412.5390.
- [69] R.V. Harlander, A. Kulesza, V. Theeuwes, T. Zirke, Soft gluon resummation for gluon-induced Higgs Strahlung, *J. High Energy Phys.* 11 (2014) 082, arXiv:1410.0217.
- [70] N. Kidonakis, Theoretical results for electroweak-boson and single-top production, *PoS DIS2015* (2015) 170, arXiv:1506.04072.
- [71] C. Muselli, M. Bonvini, S. Forte, S. Marzani, G. Ridolfi, Top quark pair production beyond NNLO, *J. High Energy Phys.* 08 (2015) 076, arXiv:1505.02006.
- [72] Y.B. Shen, R.Y. Zhang, W.G. Ma, X.Z. Li, Y. Zhang, L. Guo, NLO QCD + NLO EW corrections to WZZ productions with leptonic decays at the LHC, *J. High Energy Phys.* 10 (2015) 186, erratum: *J. High Energy Phys.* 10 (2016) 156, arXiv:1507.03693.
- [73] R. Frederix, D. Pagani, M. Zaro, Large NLO corrections in $t\bar{t}W^\pm$ and $t\bar{t}t\bar{t}$ hadroproduction from supposedly subleading EW contributions, *J. High Energy Phys.* 02 (2018) 031, arXiv:1711.02116.
- [74] W. Verkerke, D.P. Kirkby, The RooFit toolkit for data modeling, *eConf C* 0303241 (2003) MOLT007, arXiv:physics/0306116.
- [75] R. Brun, F. Rademakers, ROOT: an object oriented data analysis framework, *Nucl. Instrum. Methods Phys. Res., Sect. A* 389 (1997) 81–86.
- [76] S. Ashanujjaman, D. Choudhury, K. Ghosh, Search for exotic leptons in final states with two or three leptons and fatjets at 13 TeV LHC, in preparation.